Article

Heme Release in Myoglobin–DDAB Films and Its Role in Electrochemical NO Reduction

Matheus T. de Groot, Maarten Merkx, and Marc T. M. Koper

J. Am. Chem. Soc., **2005**, 127 (46), 16224-16232• DOI: 10.1021/ja0546572 • Publication Date (Web): 27 October 2005

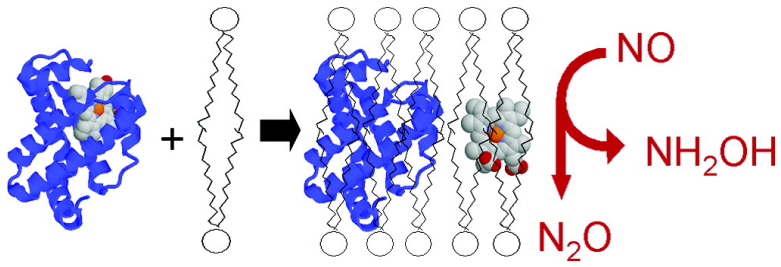

More About This Article

Additional resources and features associated with this article are available within the HTML version:

- Supporting Information
- Links to the 7 articles that cite this article, as of the time of this article download
- Access to high resolution figures
- Links to articles and content related to this article
- Copyright permission to reproduce figures and/or text from this article

View the Full Text HTML

J|A|C|S
ARTICLES
Published on Web 10/27/2005

Heme Release in Myoglobin−DDAB Films and Its Role in Electrochemical NO Reduction

Matheus T. de Groot,[†] Maarten Merkx,[‡] and Marc T. M. Koper*,[†]

Contribution from the Laboratory of Inorganic Chemistry and Catalysis, Schuit Institute of Catalysis, and Laboratory of Macromolecular and Organic Chemistry, Department of Biomedical Engineering, Eindhoven University of Technology, P.O. Box 513, 5600 MB Eindhoven, The Netherlands

Received July 13, 2005; E-mail: m.koper@chem.leidenuniv.nl

Abstract: Electrochemical nitric oxide (NO) reduction by heme groups incorporated in films of didodecyldimethylammonium bromide (DDAB) on pyrolitic graphite was investigated. It is shown that DDAB most likely induces the release of the heme group from myoglobin and therefore myoglobin−DDAB and heme−DDAB films give the same voltammetric responses. This is confirmed by UV/vis spectroscopy showing a clear shift in the Soret band of myoglobin in a DDAB solution. The electrochemical NO reduction on a heme−DDAB film at different pH values reveals the presence of pH-dependent and pH-independent NO reduction pathways. The selectivity of these pathways is probed by combining the rotating ring−disk electrode technique with online electrochemical mass spectroscopy showing that the product of the pH-independent pathway is N_2O and the product of the pH-dependent pathway is NH_2OH. The preference for one or the other pathway seems to depend on whether a proton or a NO molecule is transferred to a $Fe^{II}-NO^-$ reaction intermediate and is influenced by pH, NO concentration, and potential.

Introduction

Selective reduction of nitric oxide (NO) is a challenging catalytic problem, since four stable products can be formed: nitrous oxide (N_2O), dinitrogen (N_2), hydroxylamine (NH_2OH), and ammonia (NH_3). Enzymes such as cytochrome P450nor[1,2] are able to selectively reduce NO to N_2O, without formation of the other possible reduction products. On the other hand, on transition metals such as Pt [3−5] NO reduction often leads to a combination of N_2O, NH_2OH, and NH_3. Understanding the factors that govern selectivity in NO reduction is interesting from both a fundamental and a more applied point of view, since developing catalysts that are selective for any one of these products would be valuable.

The study of NO-reducing enzymes or their cofactors adsorbed on electrodes can provide important insights into the factors that control selectivity in NO reduction by enzymes and inorganic catalysts. In these systems the oxidation state of the enzyme or its cofactor can be directly controlled by the potential applied to the electrode. We recently studied NO reduction by heme groups directly adsorbed on pyrolitic graphite (PG)[6] and monitored its selectivity using a combination of online electrochemical mass spectroscopy (OLEMS)[7] and the rotating ring−disk electrode (RRDE) technique. Remarkably, NH_2OH was observed as the main reaction product and N_2O was observed only as a minor byproduct. This is in sharp contrast to the selectivity observed for NO reduction by heme proteins in films of didodecyldimethylammonium bromide (DDAB) on graphite. DDAB films have been employed in the immobilization of many heme proteins, notably myoglobin,[8−22] hemo-

* Corresponding author. Present address: Leiden Institute of Chemistry, Leiden University, P.O. Box 9502, 2300 RA, Leiden, The Netherlands.

[†] Laboratory of Inorganic Chemistry and Catalysis, Schuit Institute of Catalysis.

[‡] Laboratory of Macromolecular and Organic Chemistry, Department of Biomedical Engineering.

(1) Daiber, A.; Nauser, T.; Takaya, N.; Kudo, T.; Weber, P.; Hultschig, C.; Shoun, H.; Ullrich, V. *J. Inorg. Biochem.* **2002**, *88*, 343−352.
(2) Obayashi, E.; Tsukamoto, K.; Adachi, S.-i.; Takahashi, S.; Nomura, M.; Iizuka, T.; Shoun, H.; Shiro, Y. *J. Am. Chem. Soc.* **1997**, *119*, 7807−7816.
(3) de Vooys, A. C. A.; Beltramo, G. L.; van Riet, B.; van Veen, J. A. R.; Koper, M. T. M. *Electrochim. Acta* **2004**, *49*, 1307−1314.
(4) de Vooys, A. C. A.; Koper, M. T. M.; van Santen, R. A.; van Veen, J. A. R. *J. Catal.* **2001**, *202*, 387−394.
(5) Janssen, L. J. J.; Pieterse, M. M. J.; Barendrecht, E. *Electrochim. Acta* **1977**, *22*, 27−30.
(6) de Groot, M. T.; Merkx, M.; Koper, M. T. M. *J. Am. Chem. Soc.* **2005**, *127*, 7579−7586.
(7) Wonders, A. H.; Housmans, T. H. M.; Rosca, V.; Koper, M. T. M. Submitted for publication in *J. Appl. Electrochem.*
(8) Bayachou, M.; Lin, R.; Cho, W.; Farmer, P. J. *J. Am. Chem. Soc.* **1998**, *120*, 9888−9893.
(9) Nassar, A.-E. F.; Zhang, Z.; Hu, N.; Rusling, J. F.; Kumosinski, T. F. *J. Phys Chem. B* **1997**, *101*, 2224−2231.
(10) Nassar, A.-E. F.; Willis, W. S.; Rusling, J. F. *Anal. Chem.* **1995**, *67*, 2386−2392.
(11) Nassar, A.-E. F.; Zhang, Z.; Chynwat, V.; Frank, H. A.; Rusling, J. F.; Suga, K. *J. Phys. Chem.* **1995**, *99*, 11013−11017.
(12) Nassar, A.-E. F.; Rusling, J. F.; Kumosinski, T. F. *Biophys. Chem.* **1997**, *67*, 107−116.
(13) Nassar, A.-E. F.; Narikiyo, Y.; Sagara, T.; Nakashima, N.; Rusling, J. F. *J. Chem. Soc., Faraday Trans.* **1995**, *91*, 1775−1782.
(14) Nassar, A.-E. F.; Bobbitt, J. M.; Stuart, J. D.; Rusling, J. F. *J. Am. Chem. Soc.* **1995**, *117*, 10986−10993.
(15) Rusling, J. F.; Nassar, A. E. F. *J. Am. Chem. Soc.* **1993**, *115*, 11891−11897.
(16) Lin, R.; Bayachou, M.; Greaves, J.; Farmer, P. J. *J. Am. Chem. Soc.* **1997**, *119*, 12689−12690.
(17) Boussaad, S.; Tao, N. J. *J. Am. Chem. Soc.* **1999**, *121*, 4510−4515.
(18) Bayachou, M.; Elkbir, L.; Farmer, P. J. *Inorg. Chem.* **2000**, *39*, 289−293.
(19) Chen, S.-M.; Tseng, C.-C. *J. Electroanal. Chem.* **2005**, *575*, 147−160.
(20) Chen, S.-M.; Tseng, C.-C. *Electrochim. Acta* **2004**, *49*, 1903−1914.
(21) Mimica, D.; Zagal, J. H.; Bedioui, F. *J. Electroanal. Chem.* **2001**, *497*, 106−113.

10.1021/ja0546572 CCC: $30.25

globin,[21−26] catalase,[27] cytochrome P450cam,[28] cytochrome P450 CYP119,[29] cytochrome P450st,[30] and cytochrome $P450_{BM3}$,[31] and are known to increase the electrochemical response of these proteins compared to bare electrodes. The increased electrochemical response has been ascribed to the fact that proteins are able to diffuse rapidly though the DDAB layer and to the fact that DDAB inhibits the adsorption of macromolecular adsorbates that block electron transfer.[10,15] Selective N_2O formation has been reported for NO reduction by myoglobin[8] and cytochrome P450 CYP119[29] immobilized in DDAB films. Two NO reduction pathways therefore seem possible for heme-based catalysts, one leading to the formation of N_2O and the other leading to the formation of NH_2OH. Which pathway is favored apparently depends on the specific surroundings of the heme group.

To resolve the puzzling differences in selectivity between adsorbed heme groups and heme protein−DDAB films, we decided to study the selectivity of electrochemical NO reduction by myoglobin−DDAB and heme−DDAB films as a function of potential and pH. Comparing the voltammetric and catalytic responses of these films, we noted to our surprise that no significant differences between the two systems could be discerned. An explanation for this striking similarity could be the DDAB induced release of heme from myoglobin, which would transform the myoglobin−DDAB film into a heme−DDAB film. The second part of the paper presents a study of the selectivity of electrochemical NO reduction by heme−DDAB films as a function of potential and pH employing both OLEMS and RRDE. A new mechanism is presented that can explain our present results and is in accordance with previous results obtained with heme protein−DDAB films. This mechanism assumes a pH-dependent route and a pH-independent route that yield NH_2OH and N_2O, respectively, via a common $Fe^{II}-NO^-$ intermediate.

Experimental Procedures

Materials. Hemin (Fluka, 98%), equine skeletal muscle myoglobin (95%−100%, Aldrich), human hemoglobin (Aldrich), horse heart cytochrome *c* (95%, Fluka), horseradish peroxidase (Fluka) and didodecyldimethylammonium bromide (DDAB, 98%, Aldrich) were all used as received. All other chemicals were p.a. grade (Merck). Pyrolitic graphite (Carbone-Lorraine) was fabricated into homemade rotating ring−disk electrodes.[32,33] The geometric surface area of the electrodes was 0.5 cm^2. Buffer solutions were prepared with sodium acetate (pH 4−6), sodium dihydrogen phosphate monohydrate (pH 2−3, 6−8.5, 11−12), or boric acid (pH 8.5−10) combined with concentrated solutions of hydrochloric acid or caustic soda and Millipore MilliQ water (resistivity >18.2 MΩ cm). The concentration of the buffer was 0.5 M in experiments involving NO, NH_2OH, or NO_2^- reduction and 0.1 M in all other experiments. Prior to entering the electrochemical cell, nitric oxide (purity 2.5, Linde AG) was bubbled through two washing flasks filled with a 3 M KOH solution, a procedure that was found to be important to remove NO_2.[32,34] Purging the solution with NO for 10 min resulted in a saturated NO solution, which corresponds to a concentration of 2 mM as can be calculated from the Henry's law constant of 2.0×10^{-3} mol atm^{-1} at 21 °C.[35]

Electrochemical Apparatus and Procedures. An Autolab PGstat 20 potentiostat was used for cyclic voltammetry. A homemade three-electrode cell consisting of a platinum flag counter electrode, a $Hg|Hg_2SO_4$ or Ag|AgCl reference electrode, and a rotating ring−disk electrode was used. All potentials in this paper are relative to the standard calomel electrode (SCE). The rotating ring−disk electrode consisted of a pyrolitic graphite (PG) disk and a Pt ring. Experiments with rotation were conducted using a Motomatic motor generator. All solutions were deaerated by purging with argon for 10 min. All electrochemical experiments were performed at room temperature (21 ± 2 °C).

Preparation of Protein−DDAB and Heme−DDAB Films. Protein−DDAB and heme−DDAB solutions were prepared by mixing 0.5 mM protein in a 0.01 M acetate solution (pH 5) or 0.5 mM hemin in a 0.01 M borate solution (pH 10) with an equal volume of 0.01 M DDAB in a 0.1 M acetate solution (pH 5). The DDAB suspension was prepared by ultrasonication for 3 h. Prior to use, the PG electrodes were abraded using 40 μm Al_2O_3 sandpaper and ultrasonicated in Millipore MilliQ water for 5 min. The electrode was dried in a N_2 stream for 10 s. Subsequently, 5 μL of the heme/protein−DDAB solution was applied to the electrode. The electrode was dried for approximately 15 min in air, after which it was used for electrochemical experiments. Film preparation techniques, which differ from this technique, were also employed to determine their influence on the voltammetric response of the film. The differences of these techniques compared to the technique described here will be listed in the corresponding figure captions. In some cases myoglobin filtered through an YM30 filter (Amicon, 30000 MW cutoff) was used for these films.

UV/Vis Spectroscopy. UV/vis spectroscopy was performed on a Shimadzu Multispec-1501. Heme−DDAB and protein−DDAB solutions were incubated overnight using the same conditions that were used for preparing the films on PG. To allow accurate absorbance measurements, the solutions were diluted to a heme/protein concentration of 10 μM just before measuring.

Rotating Ring−Disk Electrode (RRDE) Experiments. Rotating ring−disk electrodes were constructed as described previously[32,33] and have a collection efficiency of 0.27 ± 0.03. Prior to the measurements the Pt ring was abraded together with the PG disk on 40 μm Al_2O_3 sandpaper and a protein−DDAB or heme−DDAB film was cast onto it. To remove the film, the Pt ring was cleaned by electropolishing: alternately a potential in the hydrogen evolution region (−0.8 V versus SCE) and a potential in the oxygen evolution region (1.5 V versus SCE) were applied for 5 s, a procedure which was repeated 25 times.

Online Electrochemical Mass Spectrometry (OLEMS). OLEMS measurements were performed on a Balzers Prisma QMS 200 mass spectrometer. The connection between the mass spectrometer and the cell was established through a steel capillary connected to a glass tube onto which a porous Teflon tip was attached. This tip was placed approximately 10 μm from the electrode surface. The electrode could not be rotated, hence NO was continuously bubbled through solution to enhance NO mass transfer. Baseline values measured in a solution

(22) Alatorre Ordaz, A.; Bedioui, F. *Sens. Actuators, B* **1999**, *B59*, 128−133.
(23) Lu, Z.; Huang, Q.; Rusling, J. F. *J. Electroanal. Chem.* **1997**, *423*, 59−66.
(24) Chen, X.; Hu, N.; Zeng, Y.; Rusling, J. F.; Yang, J. *Langmuir* **1999**, *15*, 7022−7030.
(25) Mimica, D.; Ringuede, A.; Agurto, C.; Bedioui, F.; Zagal, J. *Electroanalysis* **2004**, *16*, 1632−1636.
(26) Mimica, D.; Zagal, J. H.; Bedioui, F. *Electrochem. Commun.* **2001**, *3*, 435−438.
(27) Chen, X.; Xie, H.; Kong, J.; Deng, J. *Biosens. Bioelectron.* **2001**, *16*, 115−120.
(28) Zhang, Z.; Nassar, A.-E. F.; Lu, Z.; Schenkman, J. B.; Rusling, J. F. *J. Chem. Soc., Faraday Trans.* **1997**, *93*, 1769−1774.
(29) Immoos, C. E.; Chou, J.; Bayachou, M.; Blair, E.; Greaves, J.; Farmer, P. J. *J. Am. Chem. Soc.* **2004**, *126*, 4934−4942.
(30) Oku, Y.; Ohtaki, A.; Kamitori, S.; Nakamura, N.; Yohda, M.; Ohno, H.; Kawarabayasi, Y. *J. Inorg. Biochem.* **2004**, *98*, 1194−1199.
(31) Fleming, B. D.; Tian, Y.; Bell, S. G.; Wong, L.-L.; Urlacher, V.; Hill, H. A. O. *Eur. J. Biochem.* **2003**, *270*, 4082−4088.
(32) Van den Brink, F.; Visscher, W.; Barendrecht, E. *J. Electroanal. Chem.* **1983**, *157*, 283−304.
(33) Van der Plas, J. F.; Barendrecht, E. *Recl. Trav. Chim. Pays-Bas* **1977**, *96*, 133−136.
(34) de Vooys, A. C. A.; Koper, M. T. M.; van Santen, R. A.; van Veen, J. A. R. *Electrochim. Acta* **2001**, *46*, 923−930.
(35) *Lange's Handbook of Chemistry*, 14th ed.; Dean, J. A., Ed.; McGraw-Hill: London, 1992.

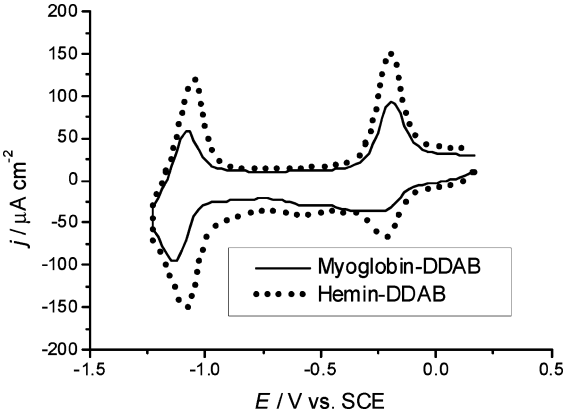

Figure 1. Cyclic voltammogram of a film cast from a solution of myoglobin−DDAB in 0.1 M sodium acetate, pH 5 (—), compared to a film cast from a solution of heme−DDAB in 0.1 M sodium acetate, pH 5 (···). Films were cast on PG and were measured in 0.1 M phosphate, pH 7.0, at a scan rate of 500 mV/s.

without NO were subtracted in NO reduction experiments. A more detailed description of the setup has been published elsewhere.[6,7]

Results

Comparison of Myoglobin−DDAB and Heme−DDAB Films. Figure 1 shows the voltammetric responses of a film cast from a myoglobin−DDAB solution and of a film cast from a heme−DDAB solution. The responses of both films resemble each other in the similarity of their peak potentials and their comparable peak sizes, which is surprising considering the differences between a large protein molecule and a small heme group. The results suggest that the peaks in both films are caused by the same species, namely a heme group in a DDAB environment. In the myoglobin−DDAB film this species could be formed by dissociation of the heme group from myoglobin (Mb).

No evidence indicating that the similarity of the Mb−DDAB film to the heme−DDAB film is a result of our particular film preparation technique was found. Results reported in the literature on differently prepared Mb−DDAB films[8,14,21,22,28] show similar peak potentials and peak sizes. To ensure that the film preparation technique does not have a significant effect on the voltammetric response, we employed different film preparation techniques with differences in protein purification (Supporting Information S1), salt concentration (Figure 4, below), pH (Supporting Information S2), solution equilibration time (Supporting Information S1), and film drying time. Apart from some differences in peak size, all films yielded a similar voltammetric response, suggesting that none of these parameters has a significant influence on the nature of the Mb−DDAB film.

The peaks in the voltammograms are due to different redox couples of the heme group. The redox couple at $E = -0.21$ V versus SCE corresponds to the Fe^{III}/Fe^{II} transition of the heme group, and the redox couple at $E = -1.12$ V versus SCE has been tentatively assigned to the Fe^{II}/Fe^{I} transition of the heme group.[14] The Fe^{III}/Fe^{II} transition is partly irreversible, which could be related to a potential-induced phase transition occurring in the DDAB film, which has been observed with atomic force microscopy.[17] Interestingly, the transition becomes more reversible with increasing scan rate, and at a scan rate of 5 V/s the couple is reversible.

To investigate further the similarities between myoglobin−DDAB and heme−DDAB films, we determined the midpoint potential of the Fe^{III}/Fe^{II} couple as a function of pH (Figure 2a) and performed electrocatalytic reduction of NO and NO_2^- (Figure 2b,c) on both films. The pH dependence of the midpoint potential is identical for both films and is in agreement with a previous study on myoglobin−DDAB films.[19] Both films also exhibit similar electrocatalytic behavior in both NO and NO_2^- reduction.[16,21] The lower activity in NO_2^- reduction for a myoglobin−DDAB film can be explained by the lower heme coverage of a myoglobin−DDAB film compared to a heme−DDAB film (Figure 1). For NO reduction this lower heme coverage does not significantly affect the catalytic wave, since NO reduction is limited by NO mass transfer. These results confirm that both films are very similar and therefore again strongly suggest that the voltammetric peaks are caused by the same species. Since it is known that DDAB forms vesicles in aqueous solution,[10] this species probably consists of a heme group incorporated in a DDAB vesicle, which can be formed after DDAB induced heme release from the protein.

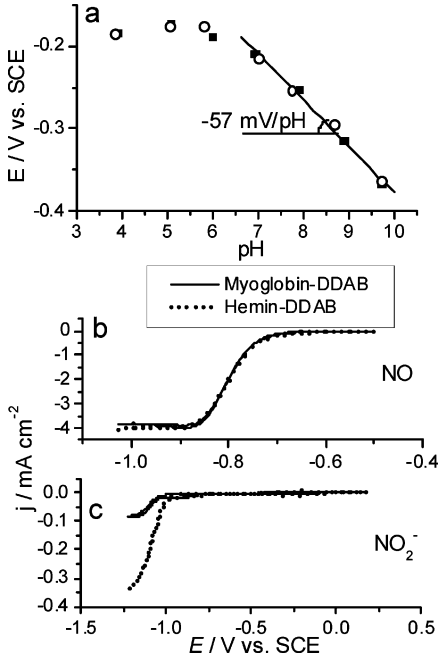

Figure 2. (a) pH dependence of midpoint potentials of redox peaks of myoglobin−DDAB film (○) and heme−DDAB film (■). Measurements were performed in 0.1 M acetate (pH 4.0−6.0), phosphate (pH 6.0−8.5), or borate (pH 8.5−10.5) at a scan rate of 500 mV/s. (b, c) Cyclic voltammograms of myoglobin−DDAB film (—) and heme−DDAB film (···) in 0.5 M sodium acetate, pH 5.0, saturated with NO (b) and in 2 mM KNO_2 in 0.5 M phosphate, pH 7.0 (c). Measurements were performed at a scan rate of 50 mV/s and a rotation rate of 16 rps.

Spectroscopic evidence for DDAB induced heme release from myoglobin can be obtained by collecting UV/vis spectra of myoglobin−DDAB and heme−DDAB solutions that were allowed to stand overnight at pH 5. Figure 3 shows that the Soret band of a myoglobin−DDAB solution is decreased and shifted (from 409 to 396 nm) compared to a myoglobin solution without DDAB. The UV/vis spectrum of a heme−DDAB solution is similar to the UV/vis spectrum of a myoglobin−DDAB solution showing the Soret (∼395 nm), Q (∼569 nm), and CT1 (∼600 nm) bands at similar wavelengths, which suggests that the species in both solutions are equivalent. This species most likely is a heme group in a micellar environment, since similar wavelengths were found for the Soret, Q, and CT1 bands of heme groups incorporated in cetyltrimethylammonium

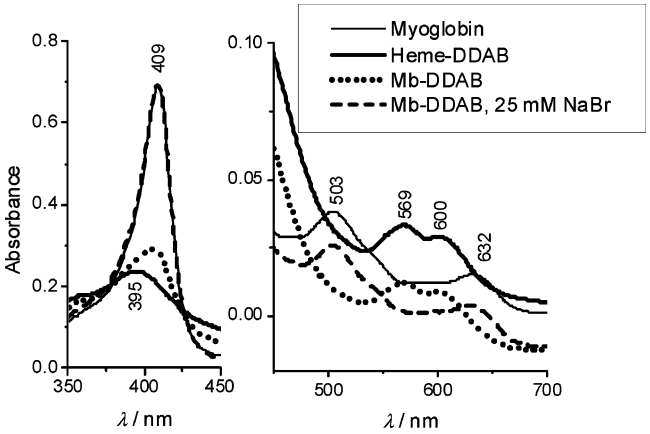

Figure 3. UV/vis spectra of myoglobin (---), myoglobin−DDAB (—), and heme−DDAB (···) solutions after overnight incubation at 4 °C in 0.1 M sodium acetate, pH 5.5, 0.25 mM myoglobin/heme, and 5 mM DDAB. Solutions were diluted 1:50 in 0.1 M sodium acetate, pH 5.5, immediately before UV/vis measurement.

(CTAB) (400, 576, and 600 nm) and Triton X-100 (398, 576, and 600 nm) micelles.[36,37] In the case of DDAB this micellar environment probably does not consist of micelles, but consists of vesicles.[38] These results show that DDAB can induce heme release from myoglobin and therefore support our voltammetric results.

Our UV/vis spectra also show that no shift of the Soret band occurs for a myoglobin−DDAB solution if 25 mM NaBr is present. Apparently the presence of salt prevents the release of heme from myoglobin in solution. This stabilizing effect of salt has also been observed for Mb−DDAB films cast on quartz and glass.[8,13−15,24,27] Interestingly, the voltammetric response of a myoglobin−DDAB film on graphite cast from a solution with salt does not significantly differ from a myoglobin−DDAB film on graphite cast from a solution without salt (Figure 4) or a heme−DDAB film on graphite. In our view it is unlikely that native myoglobin and heme give such similar voltammetric peaks in a DDAB film; therefore we think that the graphite surface is able to enhance the DDAB induced release of heme from myoglobin. Unfortunately, we cannot corroborate this with spectroscopic evidence, since pyrolitic graphite strongly adsorbs light, which makes it difficult to perform UV/vis or other forms of spectroscopy.

Increasing the pH of the myoglobin−DDAB solution gives an effect similar to the effect of salt. At pH 7 the UV/vis spectrum of the solution does not exhibit a shift in the Soret band, even in the absence of salt (Supporting Information S2a). This shows that the DDAB induced release of heme also depends on the pH of the solution. Nevertheless, on graphite the voltammetric response of the film is very similar to that of a heme−DDAB film (Supporting Information S2b), which again suggests that the peaks are caused by heme groups, the release of which is enhanced by the graphite surface. Interestingly, there is a strong influence of film drying time on the height of the peaks. A short drying time results in only small peaks, whereas a long drying time results in peak sizes similar to a film cast from a pH 5 solution. This effect could be explained in terms of a relatively slow process in which graphite enhances the DDAB induced release of heme. Short drying times abruptly abort this process, since the process cannot occur in dry films. This can explain why a similar effect of drying time was observed for a film cast from a pH 5.5 solution with salt (Figure 4), but was not observed for a film cast from a pH 5.5 solution without salt (for which heme is already released in solution).

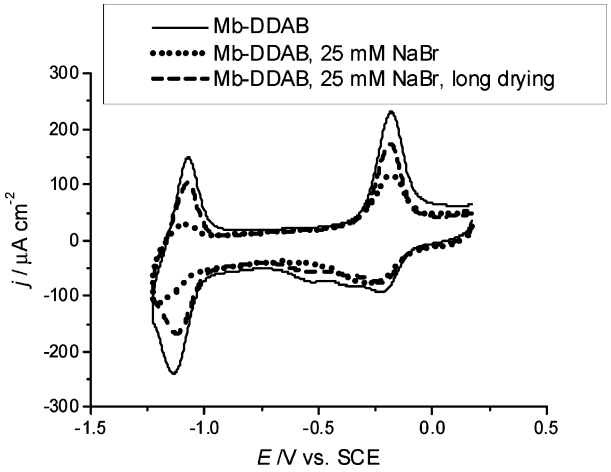

Figure 4. Cyclic voltammograms of myoglobin−DDAB films prepared according to the procedure described in the Experimental Section (—), prepared using a Mb−DDAB solution of pH 5.5 with 25 mM NaBr (···), and prepared using a solution of Mb−DDAB solution of pH 5.5 with 25 mM NaBr and slow overnight drying (---). Films were cast on PG that was abraded using 40 μm Al_2O_3 sandpaper and were measured in 0.1 M phosphate, pH 7.0, at a scan rate of 500 mV/s.

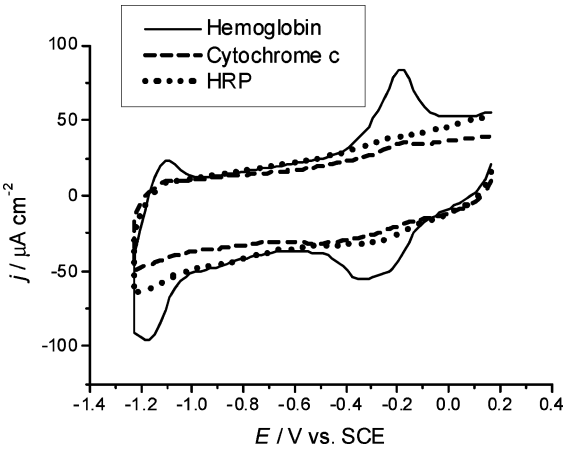

Figure 5. Cyclic voltammograms of hemoglobin−DDAB film (—), cytochrome *c*−DDAB film (···), and HRP−DDAB film (---). Films were cast on PG from protein−DDAB acetate solutions of pH 5. Measurements were performed in 0.1 M phosphate, pH 7.0, at a scan rate of 500 mV/s.

To investigate whether our findings also apply to other heme proteins, we studied the voltammetric responses of hemoglobin−DDAB, cytochrome *c*−DDAB, and horseradish peroxidase−DDAB films (Figure 5). Voltammetric peaks for the hemoglobin−DDAB film were found at potentials similar to those for the myoglobin−DDAB and heme−DDAB films, which suggests that DDAB induced heme release occurs for hemoglobin. For cytochrome *c* and horseradish peroxidase (HRP) the peaks are much smaller. This suggests that DDAB induced heme release does not readily occur for cytochrome *c* and HRP. A plausible reason for this is that the heme group is more tightly bound to the protein in HRP and cytochrome *c* than in myoglobin and

(36) Shantha, P. K.; Saini, G. S. S.; Thanga, H. H.; Verma, A. L. *J. Raman Spectrosc.* **2001**, *32*, 159−165.
(37) Shantha, P. K.; Saini, G. S. S.; Thanga, H. H.; Verma, A. L. *J. Raman Spectrosc.* **2003**, *34*, 315−321.
(38) Hamachi, I.; Honda, T.; Noda, S.; Kunitake, T. *Chem. Lett.* **1991**, 1121−1124.

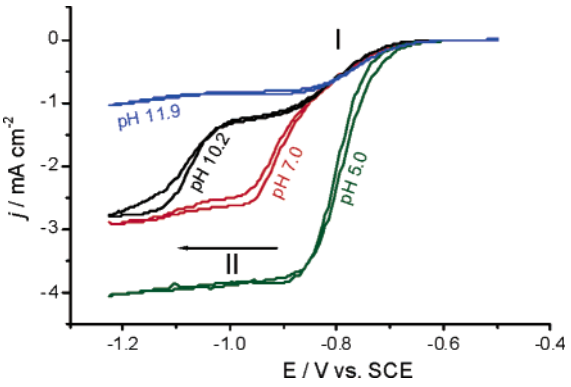

Figure 6. Cyclic voltammograms of a heme−DDAB film in 0.5 M acetate, pH 5.0; 0.5 M phosphate, pH 7.0; 0.5 M borate, pH 10.2; and 0.5 M phosphate, pH 11.9. Measurements were performed in saturated NO solution at a scan rate of 50 mV/s and a rotation rate of 16 rps.

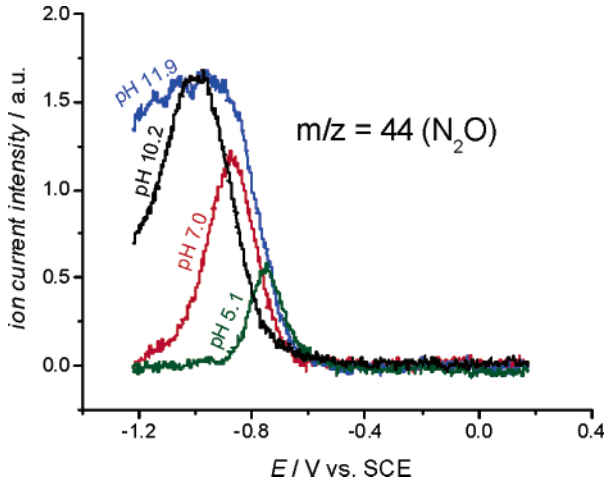

Figure 7. OLEMS measurements on a heme−DDAB film in saturated NO solution at 2 mV/s. The ion current intensity for $m/z = 44$ (N_2O) in the cathodic scan is plotted as a function of potential. Films were cast on PG and measurements were performed in 0.5 M acetate, pH 5.1; 0.5 M phosphate, pH 7.0; 0.5 M borate, pH 10.2; and 0.5 M phosphate, pH 11.9. Measurements were performed under continuous NO bubbling through the solution. Recorded current and ion current intensity for $m/z = 30$ (NO) can be found in Supporting Information S5.

hemoglobin.[39] UV/vis spectra for solutions of myoglobin, HRP, and cytochrome *c* in the presence of DDAB indeed show that cytochrome *c* and HRP are not affected by DDAB, whereas hemoglobin is (Supporting Information S3).

NO Reduction by Heme−DDAB Films. Given the similarity in voltammetric response between myoglobin−DDAB and heme−DDAB films, it is remarkable that N_2O formation has previously been reported for NO reduction by myoglobin−DDAB films and NH_2OH formation for NO reduction by hemin directly adsorbed to pyrolitic graphite. To understand the influence of the DDAB vesicles on the selectivity, we investigated NO reduction by heme−DDAB films as a function of pH and potential. Figure 6 shows the NO reduction waves for a heme−DDAB film at different pH values. The data suggest the presence of two NO reduction pathways, which can most clearly be discerned from the measurement performed at pH 10.2. At this pH reduction of NO starts around $E = -0.7$ V versus SCE, after which a plateau is reached between −0.9 and −1.0 V. A second NO reduction wave starts at $E = -1.05$ V, after which another plateau is reached. These NO reduction waves can be assigned to different pathways of NO reduction, which we will refer to as pathway I and pathway II, respectively. Pathway I starts around $E = -0.7$ V and is pH independent. Pathway II, on the other hand, is clearly pH dependent: at high pH values it is not observed at all, and with decreasing pH, it shifts to less negative potentials. Pathway I may therefore be referred to as the pH-independent pathway and pathway II as the pH-dependent pathway.

The voltammetry also suggests that the pH-independent pathway and the pH-dependent pathway have different selectivities in NO reduction. The dependence of current on rotation rate (Supporting Information S4) shows that the plateau currents are limited by NO mass transfer. The plateau currents for the pH-dependent pathway are considerably higher than those for the pH-independent pathway, which implies that more electrons are involved in the pH-dependent pathway than in the pH-independent pathway. The small differences between plateau currents at the different pH values can be explained by the dependence of the NO diffusion coefficient on the composition of the buffer solution.

The products of both pathways were determined employing online electrochemical mass spectroscopy (OLEMS)[7] and the rotating ring−disk electrode (RRDE),[40] techniques that can determine selectivity in situ. Since our voltammetric results suggested a strong influence of pH on the selectivity of NO reduction, OLEMS measurements were performed at different pH values. As was shown previously, the OLEMS setup is able to detect the formation of very small amounts of N_2O, and since the cell is purged with argon, CO_2 from air does not interfere with N_2O detection.[7] Figure 7 shows the ion current intensity for $m/z = 44$ (N_2O) as a function of potential at different pH values. The voltammetric response and the ion current intensity for $m/z = 30$ (NO) that were recorded simultaneously can be found in Supporting Information S5. Even though the electrode could not be rotated, the observed voltammetric response at different pH values is similar to Figure 6. Figure 7 shows that the amount of N_2O produced increases with increasing pH. At pH 5.1 N_2O is produced only at the start of the NO reduction and not during continuous NO reduction at lower potentials. Apparently at these lower potentials N_2O is not a reaction product. On the other hand, at pH 11.9 N_2O is observed at all potentials. When the pH-independent pathway is dominant in voltammetry, N_2O is observed in the OLEMS measurements. When the pH-dependent pathway becomes dominant, N_2O is no longer observed. This suggests that N_2O is the product of the pH-independent NO reduction pathway. The product of the pH-dependent pathway cannot be determined using OLEMS. The formation of N_2 ($m/z = 28$) was not observed, and NH_2OH and NH_3 are difficult to observe with OLEMS, because they are not gaseous and their fragmentation products have ion current intensities close to those of water.

RRDE was employed to detect the product of the pH-dependent pathway. To use the Pt ring for selectivity measurements, the voltammetric responses of the possible products (NH_2OH and NH_3) and of the reactant (NO) on Pt have to be determined. Figure 8a shows that NH_2OH and NO can be easily

(39) Messerschmidt, A.; Huber, R.; Wieghardt, K.; Poulos, T. *Handbook of Metalloproteins*; John Wiley & Sons: Chichester, 2001; Vol. 1.

(40) Bard, A. J.; Faulkner, L. R. In *Electrochemical Methods: Fundamentals and Applications*, 2nd ed.; John Wiley & Sons: New York, 1980; pp 311−367.

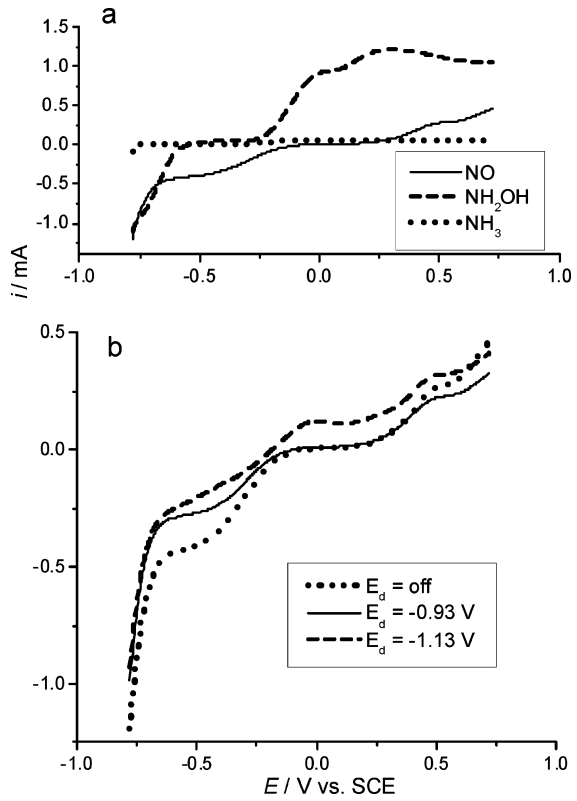

Figure 8. (a) Anodic scans of Pt ring in saturated NO solution (—), 1 mM $(NH_3OH)_2SO_4$ (---), and 2 mM NH_4Cl (···). (b) Anodic scans of Pt ring in saturated NO solution without a potential applied to the heme−DDAB disk (···), with a potential of −0.93 V applied to the heme−DDAB disk (—), and with a potential of −1.13 V applied to the heme−DDAB disk (---). Measurements were performed in 0.5 M borate, pH 10.2, at a scan rate of 50 mV/s and a rotation rate of 16 rps. The recorded current on the heme−DDAB disk was −0.51 mA at $E_d = -0.93$ V and −1.1 mA at $E_d = -1.13$ V.

distinguished by their respective oxidation and reduction waves. NH_3 oxidation on the Pt ring is negligible in comparison to NH_2OH oxidation. The voltammetric response of the Pt ring was determined during NO reduction on the heme−DDAB disk at $E_d = -0.93$ V and $E_d = -1.13$ V (Figure 8b). The measurements were performed at pH 10.2, which implies that at $E_d = -0.93$ V only the pH-independent pathway occurs, whereas at $E_d = -1.13$ V the pH-dependent pathway also occurs. For $E_d = -0.93$ V a decrease of approximately 0.14 mA was observed in the NO reduction wave on the ring, while the current on the disk was −0.51 mA. It is known that on Pt NO is reduced via a one-electron process to N_2O,[34] and combined with the collection efficiency of 0.27 ± 0.03 previously reported for this electrode,[32,33] this confirms that the pH-independent pathway also occurs via a one-electron process. Hence N_2O is the product, which is in agreement with the OLEMS results. No NH_2OH oxidation wave was observed on the ring, which confirms that NH_2OH is not a product of the pH-independent pathway. It also shows that N_2O cannot be oxidized on the Pt ring at potentials between 0 and 0.3 V versus SCE. At $E_d = -1.13$ V a clear NH_2OH oxidation wave is observed. This suggests that NH_2OH is the main product of the pH-dependent pathway. Since at $E_d = -1.13$ V part of the NO is probably still reduced by the pH-independent pathway, no quantitative information can be derived. RRDE measurements at different pH values strongly suggest that NH_2OH is the product of the pH-dependent pathway (Supporting Information S6). At lower pH values, for which the pH-dependent pathway starts at less negative potentials, an increase in the NH_2OH oxidation wave on the ring is observed already at $E_d = -0.93$ V. At high pH, for which the pH-dependent mechanism is not observed in voltammetry, no NH_2OH oxidation wave is observed, not even at $E_d = -1.13$ V. A comparison to Figure 6 shows that NH_2OH formation has a pH dependence similar to the pH-dependent pathway, suggesting that NH_2OH is the product of the pH-dependent pathway.

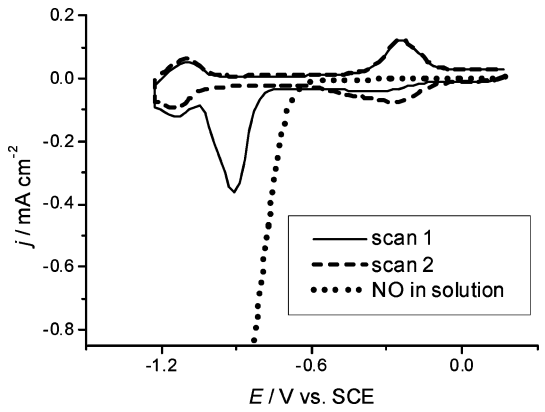

Figure 9. NO stripping voltammetry of heme−DDAB film, scan 1 (—) and scan 2 (---), compared to continuous NO reduction by heme−DDAB film (···). Measurements were performed in 0.5 M phosphate, pH 7.0, at scan rate of 500 mV/s.

Neither OLEMS nor RRDE can detect the formation of NH_3, when NH_2OH is also formed. To deduce whether NH_2OH can react further to form NH_3, the electrochemical reduction of NH_2OH by heme−DDAB films was investigated. Since no reduction of NH_2OH was observed (Supporting Information S7), N−O bond breaking by heme−DDAB films appears to be very sluggish, making it unlikely that NH_3 is a product in NO reduction by heme−DDAB films. This is in accordance with our previous study of NO reduction by adsorbed heme groups, in which we deduced that the selectivity toward NH_2OH was 100% for a pathway with a similar pH dependence.[6]

It is known that, for NO reduction on metals, N_2O formation only occurs with NO present in solution.[3,4] To investigate whether this is also the case for a heme−DDAB film, so-called NO "stripping" experiments were performed by reducing the Fe^{II}−NO adduct of the heme−DDAB film without NO present in solution. This Fe^{II}−NO adduct was formed by performing continuous NO reduction on the heme−DDAB film electrode for a short time (5 s), and subsequently transporting it to a buffer solution without NO. Figure 9 shows that NO stripping of the heme−DDAB film starts at more negative potentials than continuous NO reduction. The area under the stripping peak is 4.7×10^{-10} mol cm^{-2}, which corresponds to 2.6 electrons per heme group and implies that NH_2OH is the main product. The fact that NH_2OH and not N_2O is the product suggests that NO is stripped by the pH-dependent pathway. Apparently the pH-independent pathway does not occur without NO present in solution, similar to NO stripping on Pt, in which N_2O is also not observed.[34] The absence of the pH-independent pathway also explains why the NO stripping peak starts at more negative potentials than continuous NO reduction.

The fact that the two NO reduction pathways result in the formation of two different products makes it interesting to study their respective mechanisms in more detail. Tafel slopes[40] were

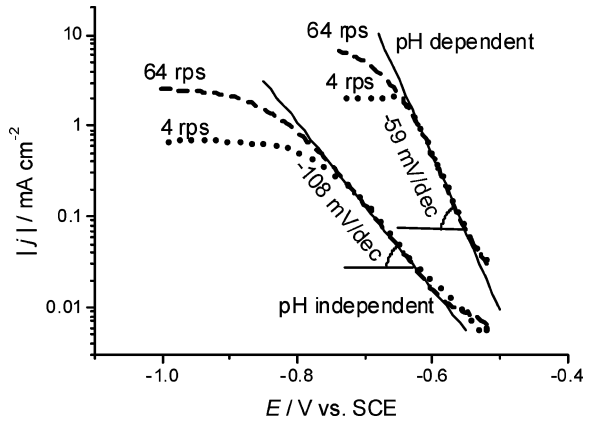

Figure 10. Absolute current density plotted on a logarithmic scale as a function of potential for NO reduction by heme−DDAB film. The Tafel slope of the pH-dependent pathway (right) was determined in 0.5 M phosphate, pH 2.5, at 64 rps (---) and 4 rps (···).The Tafel slope of the pH-independent pathway (left) was determined in 0.5 M KOH, pH 13.7, at 64 rps (---) and 4 rps (···). Plots are deduced from cathodic scans of cyclic voltammograms. Measurements were performed in saturated NO solution at a scan rate of 50 mV/s.

determined for both pathways by plotting the absolute currents measured in cyclic voltammetry on a logarithmic scale (Figure 10). The Tafel slope for the pH-dependent pathway was determined at pH 2.5 to minimize the influence of the pH-independent pathway, and the Tafel slope of the pH-independent pathway was determined at pH 13.7 to minimize the influence of the pH-dependent pathway. Figure 10 shows that the pH-dependent pathway has a Tafel slope of −59 mV/dec. A similar Tafel slope was previously observed for NO reduction by heme groups directly adsorbed on PG.[6] The Tafel slope of the pH-independent pathway is −108 mV/dec, which is reasonably close to −118 mV/dec and therefore can be interpreted in terms of a mechanism in which an electrochemical step is rate determining.[41]

The Tafel slope of −59 mV/dec observed for the pH-dependent pathway suggests the presence of an electrochemical equilibrium prior to the rate-determining step (EC mechanism).[41] This electrochemical equilibrium could be a redox couple involving the nitrosyl (NO) to nitroxyl (NO^-) transformation as was observed before.[8] We tried to detect the reversible peaks of such a redox couple by scanning at high scan rates to minimize NO reduction. At low pH we were unable to find a reversible couple for scan rates up to 50 V/s, which implies that the nitroxyl state is very unstable in acidic media. At high pH, however, a redox couple could clearly be observed for NO reduction by the heme−DDAB film (Supporting Information S8). The midpoint potential of this redox couple is independent of pH, and its value of $E = -0.91$ V versus SCE is in reasonable agreement with the value of $E = -0.87$ V reported by Bayachou et al.[8]

Discussion and Conclusions

Two main conclusions can be drawn from our study of myoglobin−DDAB and heme−DDAB films and their catalytic activity for NO reduction. First, immobilization of myoglobin−DDAB and hemoglobin−DDAB films on pyrolytic graphite induces the release of heme resulting in the formation of heme−DDAB vesicles. Second, NO reduction by these heme−DDAB vesicles can proceed via a pH-dependent pathway and a pH-independent pathway, resulting in the formation of NH_2OH and N_2O, respectively.

Our conclusion that DDAB induces release of heme in myoglobin−DDAB films is based on (i) the similar voltammetric peaks observed for myoglobin−DDAB and heme−DDAB films, (ii) the similar pH dependence of the E_m of the Fe^{III}/Fe^{II} couple for the heme−DDAB and myoglobin−DDAB films, (iii) the similar catalytic response in NO reduction for myoglobin−DDAB and heme−DDAB films, (iv) the shift in wavelength of the Soret band for myoglobin in a DDAB solution and the similar wavelengths observed for the Soret, Q, and CT1 bands for a myoglobin−DDAB solution compared to a heme−DDAB solution, and (v) the observation that the voltammetric peaks are much smaller for DDAB films of heme proteins such as cytochrome *c* and HRP, in which the heme group is more tightly bound to the protein.

Various other studies also showed that interactions between surfactants and myoglobin can induce the release of heme groups,[42−44] resulting in the incorporation of the heme groups in micelles.[43] In addition, it is known that heme groups incorporated in micelles can exhibit a strong voltammetric response.[45−47] Furthermore, similar redox potentials for the Fe^{III}/Fe^{II} couple have been reported for different heme proteins incorporated in DDAB films,[21] and often these potentials do not correspond to the redox potentials of the proteins in solution.[28] In addition, the charge under the voltammetric peaks corresponds to more than one protein monolayer, which combined with the fact that the peaks are reversible up to scan rates of more than 100 mV/s[23,28] would suggest an almost improbably fast protein diffusion within the DDAB layer.

Our results indicate that the use of UV/vis spectroscopy on films cast on quartz or glass can sometimes be insufficient to determine whether the voltammetric peaks observed are caused by the native protein. A valuable extra control experiment is the comparison of the voltammetric response of the protein incorporated in the film to the voltammetric response of the cofactor incorporated in the same film. This control experiment is not only useful for heme proteins in DDAB films, but might also be of value for heme proteins incorporated in other films.[48−53]

Our results show two NO reduction pathways on heme−DDAB films: a pH-independent pathway resulting in the formation of N_2O and a pH-dependent pathway resulting in the formation of NH_2OH. Although it is tempting to relate the pH-dependent pathway to the possible Fe^{II}/Fe^{I} couple, the potential

(41) Vetter, K. J. In *Elektrochemische Kinetik*; Springer-Verlag: Berlin, 1961; pp 302−357.
(42) Blauer, G.; Harmatz, D.; Zvilichovsky, B. *FEBS Lett.* **1973**, *34*, 344−346.
(43) Kanti Das, T.; Mazumdar, S.; Mitra, S. *J. Chem. Soc., Chem. Commun.* **1993**, 1447−1448.
(44) Tofani, L.; Feis, A.; Snoke, R. E.; Berti, D.; Baglioni, P.; Smulevich, G. *Biophys. J.* **2004**, *87*, 1186−1195.
(45) Das, D. K.; Bhattaray, C.; Medhi, O. K. *J. Chem. Soc., Dalton Trans.* **1997**, 4713−4718.
(46) Das, D. K.; Medhi, O. K. *J. Chem. Soc., Dalton Trans.* **1998**, 1693−1698.
(47) Das, D. K.; Medhi, O. K. *J. Inorg. Biochem.* **1998**, *70*, 83−90.
(48) Liu, X.; Zhang, W.; Huang, Y.; Li, G. *J. Biotechnol.* **2004**, *108*, 145−152.
(49) Wang, Q.; Lu, G.; Yang, B. *Langmuir* **2004**, *20*, 1342−1347.
(50) Nadzhafova, O. Y.; Zaitsev, V. N.; Drozdova, M. V.; Vaze, A.; Rusling, J. F. *Electrochem. Commun.* **2004**, *6*, 205−209.
(51) Huang, H.; He, P.; Hu, N.; Zeng, Y. *Bioelectrochemistry* **2003**, *61*, 29−38.
(52) Shen, L.; Huang, R.; Hu, N. *Talanta* **2002**, *56*, 1131−1139.
(53) Tang, J.; Jiang, J.; Song, Y.; Peng, Z.; Wu, Z.; Dong, S.; Wang, E. *Chem. Phys. Lipids* **2002**, *120*, 119−129.

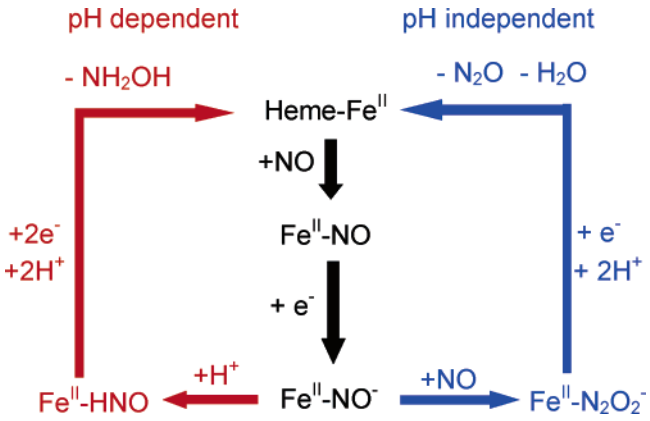

Figure 11. Mechanisms of the two pathways for NO reduction observed for heme−DDAB film cast on PG.

of this Fe^{II}/Fe^{I} couple is independent of pH (data not shown) and therefore this is unlikely. Therefore we postulate different mechanisms for both pathways in Figure 11 based on their products and the observed Tafel slopes. For the pH-independent pathway the Tafel slope of −108 mV/dec suggests that the first electron transfer is rate determining. Most likely this is the reduction of the Fe^{II}−NO adduct formed by reaction of Fe^{II}−heme with NO. Since the pathway is pH independent, a proton transfer is not involved in this step; hence Fe^{II}−NO^- must be the product. However, a change in the rate-determining step might occur at lower NO concentrations and under conditions where NO mass transfer is rate limiting. In these cases the reaction of the Fe^{II}−NO^- adduct with NO might become rate determining. Such a change in the rate-determining step would explain why the Fe^{II}−NO/Fe^{II}−NO^- couple can be observed at high scan rates at high pH. A similar change of rate-determining step with NO concentration has also been reported for the enzyme cytochrome P450nor.[1] For the pH-dependent pathway the Tafel slope of −59 mV/dec suggests an electrochemical equilibrium followed by a chemical rate-determining step. The electrochemical equilibrium could be the Fe^{II}−NO/Fe^{II}−NO^- couple, and the chemical rate-determining step that follows might be the proton transfer that results in the formation of Fe^{II}−HNO. This is supported by the pH dependence of the pathway. On the basis of this mechanism, one would expect to be able to observe a Fe^{II}−NO/Fe^{II}−NO^- couple at high scan rates. Unfortunately, our maximum scan rate (1000 V/s) was too slow to observe the couple. This suggests that even though the proton transfer is rate determining, it is still very rapid at low pH values. Fe^{III}−Fe^-

Figure 11 suggests that there are three factors that govern which NO reduction pathway occurs. These are the pH of the solution, which determines whether a proton transfer occurs to the Fe^{II}−NO^- adduct, the NO concentration in solution, which determines the rate of the reaction of the Fe^{II}−NO^- adduct with NO, and the potential of the electrode, which determines the concentration of the Fe^{II}−NO^- adduct. Even though the Fe^{II}−NO^- adduct is an intermediate in both pathways, an increase in the concentration of the Fe^{II}−NO^- adduct can result in a change from the pH-independent pathway to the pH-dependent pathway under conditions where the reaction is limited by NO mass transfer.

An attractive feature of the mechanisms we propose for NO reduction by heme−DDAB films is that they can explain the results for NO reduction by myoglobin−DDAB films obtained by other groups.[8,26] We consider this another confirmation of our conclusion that myoglobin−DDAB films and heme−DDAB films are equivalent. Previous studies on myoglobin−DDAB films show a similar interpretation of results in terms of the pH-independent pathway, but they could not clearly explain certain parts of the results, which we would now ascribe to the pH-dependent pathway. First, it was observed in these studies that the reversible Fe^{II}−NO/Fe^{II}−NO^- couple could only be found at high pH values and that the lifetime of the Fe^{II}−NO^- adduct decreases with pH.[8] We can now ascribe this to the fact that the Fe^{II}−NO^- adduct reacts further to NH_2OH. Second, a second NO reduction wave was also observed in previous studies.[26] This peak was ascribed to a second electron transfer, but we can now readily ascribe it to the pH-dependent pathway. The fact that NH_2OH was not previously reported as a product in NO reduction by a protein−DDAB film[8] is probably due to the fact that the electrolysis experiments in which the selectivity of the reaction was determined were performed at a potential where the pH-independent pathway dominates.

The presence of two different NO reduction pathways has also been observed for heme enzymes. The cytochrome P450nor selectively reduces NO to N_2O,[1] whereas the cytochrome *c′* nitrite reductase[54] selectively reduces nitrite to NH_3. Although the substrate of cytochrome *c′* nitrite reductase is nitrite instead of NO, the reaction occurs via a heme−NO intermediate similar to NO reduction by the cytochrome P450nor. The different selectivity of both enzymes therefore confirms that there are at least two pathways in heme−NO reduction.

The two different pathways can also explain the remarkable difference in selectivity previously reported for NO reduction by adsorbed heme (NH_2OH) as compared to NO reduction by heme protein−DDAB films (N_2O). For the heme−DDAB film our results demonstrate that NO reduction does not necessarily result in the formation of N_2O, but can also result in the formation of NH_2OH. For adsorbed heme we previously reported NH_2OH as the main product, but we did observe N_2O as a minor byproduct.[6] This suggests that in both systems the two NO reduction pathways presented in Figure 11 can occur. However, both systems are also distinctly different. At pH 7 the amount of N_2O we observed for a heme−DDAB film is more than 10 times larger than the amount of N_2O reported previously for adsorbed heme. This suggests that the specific surroundings of the heme group influence important parameters such as the potential of the Fe^{II}−NO/Fe^{II}−NO^- couple, the rate of protonation of the Fe^{II}−NO^- intermediate, and the local NO concentration (which has been suggested to be higher in DDAB films than in aqueous buffer solutions[8]), parameters that determine the preference for one or the other pathway.

Acknowledgment. This work was supported by the National Research School Combination Catalysis (NRSC-C).

Supporting Information Available: Voltammograms of Mb−DDAB films prepared in different ways, UV/vis spectra of hemoglobin, cytochrome *c*, and horseradish peroxidase in the presence of DDAB, cyclic voltammograms of NO reduction

(54) Einsle, O.; Messerschmidt, A.; Huber, R.; Kroneck, P. M. H.; Neese, F. *J. Am. Chem. Soc.* **2002**, *124*, 11737−11745.

by a heme−DDAB film at different rotation rates, the current and ion current intensity signal for $m/z = 30$ (NO) recorded during the OLEMS measurements, rotating ring−disk experiments performed at pH 5.1, pH 6.9, and pH 11.9, a cyclic voltammogram of a heme−DDAB film in the presence of hydroxylamine, and cyclic voltammograms of a heme−DDAB film at high scan rates in basic solution. This information is available free of charge via the Internet at http://pubs.acs.org.

JA0546572